CRYSTAL GROWTH & DESIGN

Subscriber access provided by University of South Dakota

Article

Structure-Property Relationship in Energetic Cationic Metal–Organic Frameworks: New Insight for Design of Advanced Energetic Materials

Yao Du, Hui Su, Teng Fei, Baoping Hu, Jichuan Zhang, Shenghua Li, Siping Pang, and Fude Nie

Cryst. Growth Des., **Just Accepted Manuscript** • DOI: 10.1021/acs.cgd.8b00640 • Publication Date (Web): 21 Aug 2018

Downloaded from http://pubs.acs.org on August 21, 2018

Just Accepted

“Just Accepted” manuscripts have been peer-reviewed and accepted for publication. They are posted online prior to technical editing, formatting for publication and author proofing. The American Chemical Society provides “Just Accepted” as a service to the research community to expedite the dissemination of scientific material as soon as possible after acceptance. “Just Accepted” manuscripts appear in full in PDF format accompanied by an HTML abstract. “Just Accepted” manuscripts have been fully peer reviewed, but should not be considered the official version of record. They are citable by the Digital Object Identifier (DOI®). “Just Accepted” is an optional service offered to authors. Therefore, the “Just Accepted” Web site may not include all articles that will be published in the journal. After a manuscript is technically edited and formatted, it will be removed from the “Just Accepted” Web site and published as an ASAP article. Note that technical editing may introduce minor changes to the manuscript text and/or graphics which could affect content, and all legal disclaimers and ethical guidelines that apply to the journal pertain. ACS cannot be held responsible for errors or consequences arising from the use of information contained in these “Just Accepted” manuscripts.

ACS Publications

is published by the American Chemical Society. 1155 Sixteenth Street N.W., Washington, DC 20036

Published by American Chemical Society. Copyright © American Chemical Society. However, no copyright claim is made to original U.S. Government works, or works produced by employees of any Commonwealth realm Crown government in the course of their duties.

Structure-Property Relationship in Energetic Cationic Metal–Organic Frameworks: New Insight for Design of Advanced Energetic Materials

Yao Du,[†] Hui Su,[†] Teng Fei,[†] Baoping Hu,[†] Jichuan Zhang,[†] Shenghua Li,[*,†] Siping Pang,[*,†] and Fude Nie[‡]

[†]School of Materials Science & Engineering, Beijing Institute of Technology, Beijing 100081, P. R. China

[‡]Institute of Chemical Materials, China Academy of Engineering Physics (CAEP), Mianyang, Sichuan 621900, P. R. China

ABSTRACT: Understanding the structure-property relationship in a material is of great importance in material science. To study the effect of ligand backbones and anionic groups on the properties of energetic cationic metal-organic frameworks (CMOFs) and to disclose their structure-property relationships, we designed and synthesized a series of CMOFs based on either 4,4'-bi-1,2,4-triazole (btrz) or its azo analogous, 4,4'-azo-1,2,4-triazole (atrz) as ligand, and either perchlorate [ClO_4^-] or nitroformate [$C(NO_2)_3^-$, NF$^-$] anion as extra-framework anion. Surprisingly, the effect of ligand backbones on the CMOFs is inverse that of the backbones on traditional energetic compounds, while the effect of the anionic groups follows the traditional group law. We found that btrz-based CMOFs exhibit higher densities and better chemical and thermal stabilities than those of their corresponding atrz-based CMOFs, although btrz has a lower density and a lower stability than atrz. In particular, the density of **btrz-Fe** is more than 0.11 g cm^{-3} higher than that of its atrz-based analogue (**atrz-Fe**). Moreover, the decomposition temperature of **btrz-Zn** (363 °C) is 80 °C higher than that of **atrz-Zn**, even higher than that of 1, 3, 5-triamino-2, 4, 6-trinitrobenzene (TATB), making it a potential heat-resistant explosive. The effect mechanisms were also discussed according to the experimental results. This investigation is significant for understanding the structure-property relationship in energetic CMOFs. Moreover, it also brings about new design rules for future high-performance energetic materials.

INTRODUCTION

The study of structure-property relationship is one of the key pillars of various functional materials such as electronic and photonic materials, organic semiconductors, pharmaceuticals, batteries, gas absorbent, and catalysts since it provides insight and guidance that suggest paths to future advances.[1-6] Especially, for energetic materials including explosives, propellants, and pyrotechnics, which have extensive applications in military and civilian fields, understanding the basic principles of their structure-property relationships would allow for better design and achievement of desired properties.[7] In general, the structure of traditional energetic compounds such as TNT, RDX, and CL-20 is composed of two parts: backbones (e.g., aromatic rings, strain-caged rings, and nitrogen-rich heterocyclic rings) and energetic groups (e.g., NH_2, NO_2, and N_3, **Scheme 1**). Their structure-property relationships and the effect of the backbones and energetic groups on the energetic properties have been well documented.[8-11] An energetic compound with a denser backbone usually results in its higher density and higher energy, while introducing a higher energy group into the same energetic backbone also improves both. For example, RDX is more energetic than TNT since it contains a denser heterocyclic backbone compared to the benzene backbone of TNT, which can produce additional energy from the combustion of more C-N bonds. CL-20 has the highest energy among the three energetic compounds because of its dense strained backbone.[12] Meanwhile, since the nitro group has a higher energy than the amino group, and the amino group possesses a higher energy compared to the H atom, introducing these groups into the same tetrazole backbone shows gradually increasing orders in density and energy as follow: tetrazole < 5-amino-tetrazole (5-AT) < 5-nitro-tetrazole (5-NT).[13]

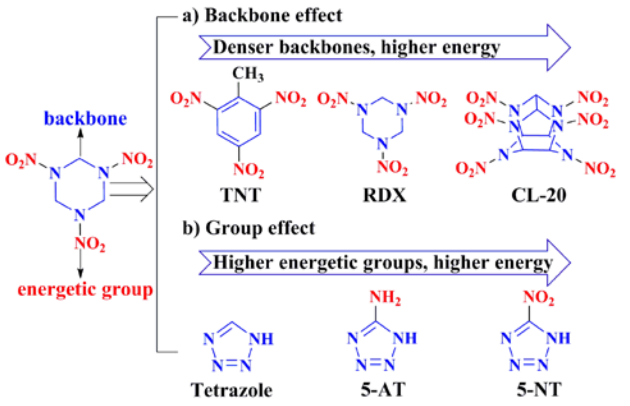

Scheme 1. Backbone effect (a) and group effect (b) of traditional energetic compounds.

As an emerging class of energetic materials, energetic cationic metal-organic frameworks (CMOFs) have become a research hotspot in recent years owing to their favorable thermal stabilities, high densities, and high heats of detonation,[14-18] which present promising applications in pyrotechnics, primary explosives, explosives, and energetic composites.[19-22] Their positive frameworks can be constructed using energetic nitrogen-rich ligands and metal ions. The extra-framework of energetic anions such as ClO_4^- and NO_3^- occupy the framework channels as mobile anions, which are usually uncoordinated to metal centers. Based on their structural features, energetic CMOFs are also regarded in two parts (metal ions usually have little influences on the detonation properties of metal-organic frameworks):

backbones (ligands) and energetic groups (energetic anions, **Scheme 2**), similar to traditional energetic compounds. Although numerous CMOFs with fantastic topological structures have been synthesized through choosing various ligand backbones and anionic groups,[23, 24] the effect of both on energetic properties remain unclear. Therefore, to properly tailor the structures of energetic CMOFs for desired properties, systematically investigating their structure-property relationships is imperative.

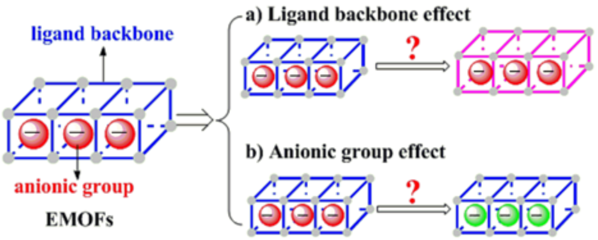

Scheme 2. Ligand backbone effect (a) and anionic group effect (b) of energetic CMOFs.

Here, we rationally designed an energetic CMOF-based model system to disclose the structure-property relationship. The model includes two kinds of CMOFs (btrz-based CMOFs and atrz-based CMOFs), which are based on either 4,4'-bis-triazole (btrz) or its azo analogous 4,4'-azo-triazole (atrz) as ligands. Compounds btrz and atrz were chosen as typical ligands for the following reasons: (1) btrz and atrz are easily available and possess strong coordination abilities and same coordination modes,[21, 25, 26, 40] which contribute to the construction of CMOFs with similar structures, thus conveniently enabling the study of the effect of ligand backbones on their properties.[26-28] (2) The structure-property relationships of btrz and atrz are well-documented (**Scheme 3**),[27, 29] which would be helpful to conduct a comparative study between the properties of btrz-based CMOFs and atrz-based CMOFs. (3) They possess high nitrogen contents (61.74% for btrz and 68.27% for atrz) and high heats of formation (531 kJ mol^{-1} for btrz and 878 kJ mol^{-1} for atrz), which could contribute to the development of high-energy CMOFs. Additionally, either perchlorate [$\mathrm{ClO_4^-}$] or nitroformate anion [$\mathrm{C(NO_2)_3^-}$, NF$^-$] was employed as an extra-framework energetic anion because these two anions have different densities [e.g., 2.52 g cm^{-3} for $\mathrm{KClO_4}$ vs 2.22 g cm^{-3} for $\mathrm{KC(NO_2)_3}$] and thermal stabilities [e.g., the decomposition temperature of $\mathrm{KC(NO_2)_3}$ is 83 °C, while that of $\mathrm{KClO_4}$ is 400 °C],[30, 31] which allows the assessment of the effect of anionic groups. To further investigate the generality of the effect of ligand backbones and anionic groups, three different metal ions (Zn, Cu, and Fe) were selected as metal centers to construct different isostructural CMOFs.

Based on the above design strategy, a series of energetic CMOFs with similar structures but different ligand backbones and anionic groups (**btrz-Zn**: $\{[\mathrm{Zn(btrz)_3}](\mathrm{ClO_4})_2\}_n$; **btrz-Cu**: $\{[\mathrm{Cu(btrz)_3}](\mathrm{ClO_4})_2\}_n$; **btrz-Fe**: $\{[\mathrm{Fe(btrz)_3}](\mathrm{ClO_4})_2\}_n$; **Zn-NF**: $\{[\mathrm{Zn(btrz)_3}](\mathrm{C(NO_2)_3})_2\}_n$; **Cu-NF**: $\{[\mathrm{Cu(btrz)_3}](\mathrm{C(NO_2)_3})_2\}_n$; **atrz-Zn**: $\{[\mathrm{Zn(atrz)_3}](\mathrm{ClO_4})_2\}_n$; **atrz-Cu**: $\{[\mathrm{Cu(atrz)_3}](\mathrm{ClO_4})_2\}_n$; **atrz-Fe**: $\{[\mathrm{Fe(atrz)_3}](\mathrm{ClO_4})_2\}_n$) were synthesized and characterized by IR spectroscopy, powder X-ray diffraction (PXRD), and single-crystal x-ray diffraction. The effects of ligand backbones and anionic groups on the properties of CMOFs such as density, chemical stability, thermal stability, sensitivity, and heat of detonation were studied. In addition, the effect mechanisms were also discussed according to the experimental results. This study is the first example for the systematic investigation of structure-property relationship in energetic CMOFs.

Results and discussion

1. Effect of ligand backbone on the properties of energetic CMOFs

(1) Synthesis and Structure. To exploring the effect of ligand backbones on the properties of CMOFs, three btrz-based CMOFs (**btrz-Zn**, **btrz-Cu**, and **btrz-Fe**) and their corresponding atrz-based CMOFs (**atrz-Zn**, **atrz-Cu**, and **atrz-Fe**) were prepared from hydrothermal reactions of btrz or atrz with their metal salts with the same perchlorate anions, respectively (**Scheme 3** and **Scheme S2**). These materials can be synthesized with high yields and purities; their phase purities were established by comparison of their observed and simulated powder X-ray diffraction (see **Figure S1-S2**).

Single-crystal X-ray diffraction revealed that btrz-based CMOFs are isostructural as well as atrz-based CMOFs. Furthermore, all six CMOFs have the same extra-framework perchlorate anion, display similar structures, and have the same asymmetric units $\{[\mathrm{ML_3}](\mathrm{ClO_4})_2$; M= Zn, Cu, or Fe; L= atrz or btrz$\}$ of one metal atom, three ligands, and two non-coordinated $\mathrm{ClO_4^-}$ anions. Moreover, the central metal ions in these CMOFs are coordinated by six nitrogen atoms from six different ligand molecules (**Figure 1a**, **b** and **Figure S9-12a**). Each ligand molecule acts as a bidentate bridge and connects two adjacent metal centers, thus extending into a similar 3D cationic framework structure (**Figure 1e**, **f** and **Figure S9-12b**). The frameworks possess one-dimensional (1D) channels, which were filled with charge-balanced disordered $\mathrm{ClO_4^-}$ anions. In addition, the oxygen atoms of the $\mathrm{ClO_4^-}$ anions and the C-H groups of the triazole rings participate in the formation of several C-H•••O hydrogen bonding.

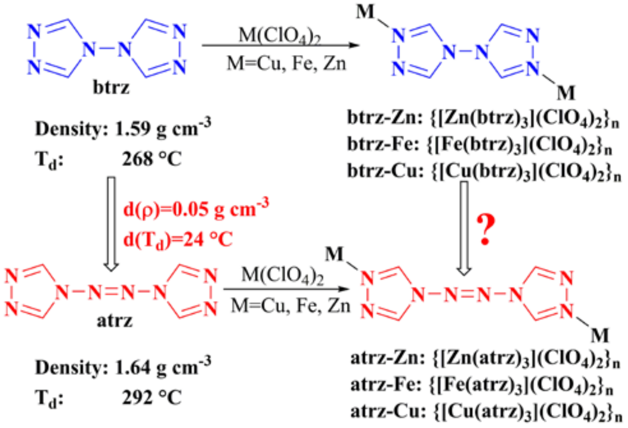

Scheme 3. Synthesis of btrz-based CMOFs and atrz-based CMOFs with the same extra-framework $\mathrm{ClO_4^-}$ anions.

However, there are a few significant differences between the btrz-based CMOFs and their corresponding atrz-based CMOFs. To describe them in detail, we took **btrz-Zn** and **atrz-Zn** as typical examples and made a comparison. The differences were found as follows: (1) In **btrz-Zn**, the two triazolyl rings of btrz are nearly perpendicular to each other since they are linked via the rotatable N–N single bond, and the twisting angle between them is 81.946(3)° (**Figure 1d**). Conversely, in **atrz-Zn**, two triazolyl rings and an azo group of the atrz ligand are nearly coplanar to each other due to the formation of a large conjugated system between the two aromatic triazolyl rings and the azo group, and the twisting angle between two triazolyl rings is only 2.664(3)° (**Figure 1c**). Therefore, **btrz-Zn** exhibits more flexible frameworks than **atrz-Zn** because its ligands are more flexible. (2) The Zn^{II}-N bond lengths increases from 2.153(3) Å in **btrz-Zn** to 2.169(2) Å in **atrz-Zn** (**Table S3**). Thus, the btrz ligand possesses stronger coordination stability than the atrz ligand. (3) The C-H•••O hydrogen bonding distances between the oxygen atoms of the ClO$_4^-$ anions and the C-H groups of the triazole rings are about 2.6333(139) Å in **btrz-Zn**, while those in **atrz-Zn** are about 2.7444(98) Å (**Table S4**), suggesting that **btrz-Zn** has stronger hydrogen-bonding interactions than **atrz-Zn**. (4) **btrz-Zn** possesses 1D channels with inner diameter of about 5.6 Å, while that in **atrz-Zn** has about 6.2 Å (Figure 1e, f). Moreover, PLATON calculations[32] showed that the total empty volumes of the cationic framework reduced from 34.1% in **atrz-Zn** to 33.4 % in **btrz-Zn**. It is possible that the length of the btrz ligand (5.5 Å) is shorter than that of the atrz ligand (7.7 Å, **Figure 1c** and **d**). In addition, the btrz ligand has rotatable N-N single bonds, which leads to **btrz-Zn** having smaller channels and lower empty volumes.

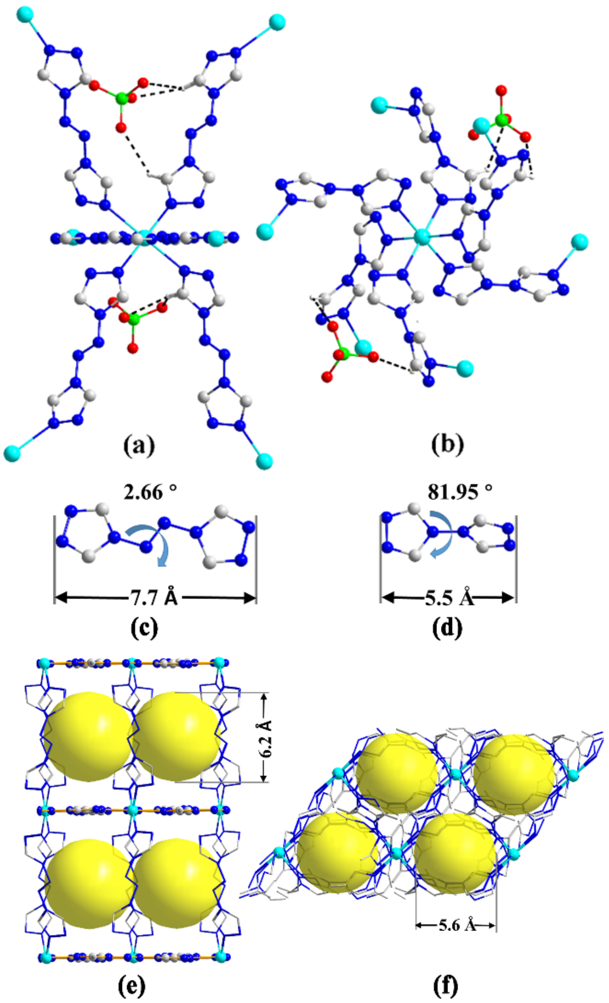

Figure 1. Coordination environment of Zn in **atrz-Zn** (a). Coordination environment of Zn in **btrz-Zn** (b). Structure for ligand atrz in **atrz-Zn** (c). Structure for ligand btrz in **btrz-Zn** (d). 3D frameworks of btrz-Zn (e). 3D frameworks of **atrz-Zn** (f). Some charge-balancing anions, hydrogen atoms, and guest water are omitted for clarity. The large spheres indicate the size of the voids.

(2) **Density.** Density is one of the most important physical properties of an energetic material. For example, the detonation velocity of an explosive is proportional to its density, and the detonation pressure is proportional to the square of its density.[33] The densities of as-synthesized btrz-based CMOFs and atrz-based CMOFs after desolvation were measured using an automatic gas pycnometer. The densities of **btrz-Zn, btrz-Cu,** and **btrz-Fe** are 1.81, 1.83 and 1.82 g cm^{-3}, while those of **atrz-Zn**, **atrz-Cu** and **atrz-Fe** are 1.72, 1.74 and 1.71 g cm^{-3}, respectively. Surprisingly, although btrz has a lower density than atrz (1.64 g cm^{-3} for atrz vs 1.59 g cm^{-3} for btrz), btrz-based CMOFs display higher densities than their corresponding atrz-based CMOFs (**Figure 2**). This contradicts the traditional density law, which states that as the backbone becomes denser, its energetic compound has a higher density. In particular, the density of **btrz-Fe** is more than 0.11 g cm^{-3} higher than that of its azo-based analogue (**atrz-Fe**). The relatively high densities of btrz-based CMOFs could be attributed to their smaller channels (e.g., 5.6 Å for **btrz-Zn** *vs* 6.2 Å for **atrz-Zn**; 5.5 Å for **btrz-Fe** *vs* 6.3 Å for **atrz-Fe**) and lower porosity (e.g., 33.4% for **btrz-Zn** vs 34.1% for **atrz-Zn**; 33.6% for **btrz-Fe** vs 34.1% for **atrz-Fe**), which lead to a denser layer-by-layer stacking. Traditionally, the densities of energetic compounds mainly rely on backbones and energetic groups.[8-11] However, for energetic CMOFs, the size of channels and the total empty volume of the frameworks also significantly influence density, which is scarcely displayed in traditional energetic compounds.

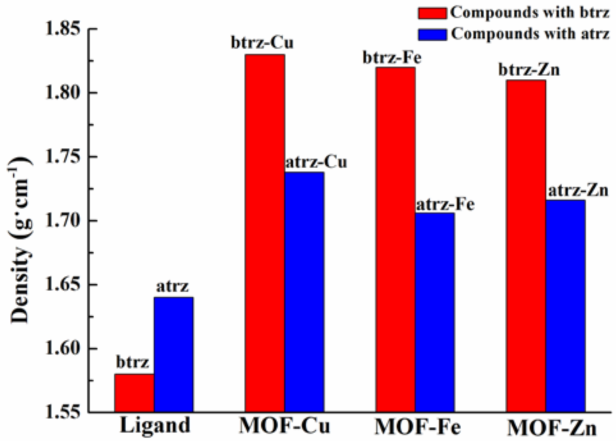

Figure 2. Densities comparison for btrz, atrz and their atrz-based CMOFs and btrz-based CMOFs with the same extra-framework ClO$_4^-$ anions.

(3) **Stability.** Stability is also a crucial property for the practical application of energetic materials. These CMOFs were stable in air and common organic solvents such as ethanol, methanol, DMSO, and DMF. To investigate their chemical stabilities, each sample was dispersed in aqueous solutions with different pH values (1-14). Subsequently, the samples were thoroughly washed with water and dried before

characterization. As shown in **Figures 3** and **S3**, the PXRD patterns of these materials were almost similar in aqueous solutions of pH 1 to 10. However, in a pH 14 aqueous solution, the diffraction intensities of atrz-based CMOFs clearly decreased and some new peaks appeared, while those of btrz-based CMOFs maintained intact. For example, the diffraction intensity corresponding to the (1, 0, 1) crystallographic plane at 15.39° in 2θ (**Figure 3a**, peak a) of **atrz-Zn** in a pH 14 aqueous solution decreased from 10000 to 1000 cps, and a new peak corresponding to the (1, 3, -1) crystallographic plane at 19.18° in 2θ (**Figure3a**, peak b) became particularly prominent. In contrast, the diffraction pattern and intensities of **btrz-Zn** were almost unchanged following the same pH change (**Figure 3b**). These results demonstrated that btrz-based CMOFs exhibit better chemical stabilities in both acid and base solutions, allowing their applications under different conditions. Moreover, although some MOFs have been previously reported to have water tolerance or chemical stability in acidic or basic media, very few MOFs were found to be stable in both.[34-36]

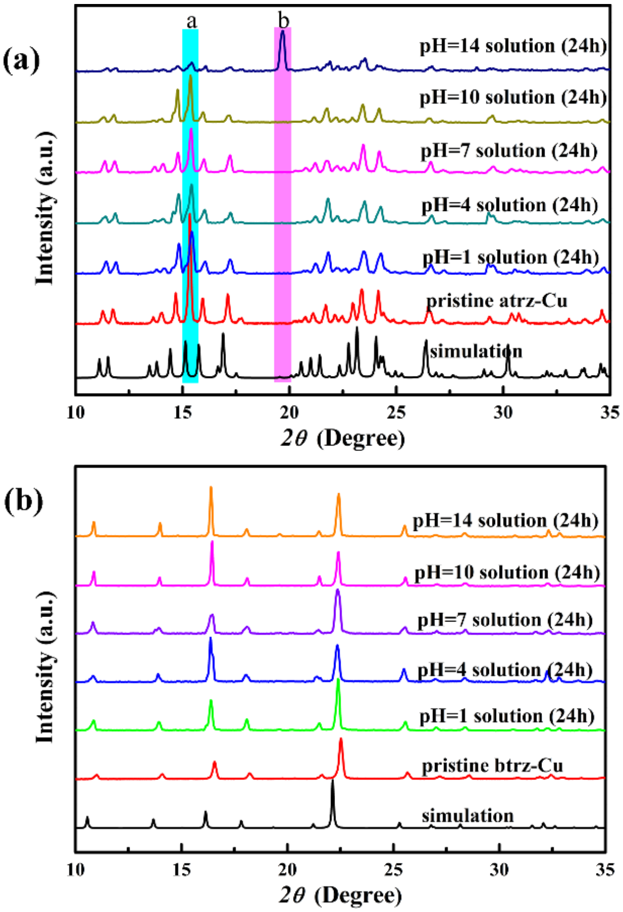

Figure 3. PXRD profiles for simulated and experimental **atrz-Cu** (a) and **btrz-Cu** (b) samples soaked in aqueous solutions with pH values of 1, 4, 7, 10 and 14 for 24 h.

Their thermal stabilities were measured by differential scanning calorimetry (DSC) and thermogravimetric (TG) analysis under N_2 atmosphere. As shown in **Figure 4**, all the CMOFs display high thermal stabilities. The decomposition temperatures of **btrz-Cu** and **btrz-Fe** are 321 and 312 °C, while those of **atrz-Cu** and **atrz-Fe** are 274 and 271 °C, respectively. Interestingly, **btrz-Zn** possesses an extremely high thermal stability with an onset decomposition temperature of 363 °C, even higher than 1,3,5-triamino-2,4,6-trinitrobenzene (TATB, 318 °C),[37] one of the most famous insensitive and heat-resistant explosives known. Thus, **btrz-Zn** could be a potential heat-resistant explosive. Furthermore, btrz-based CMOFs also exhibited higher thermal stabilities than those of their atrz-based counterparts (**Figure S4-S6**), which is inverse of the relationship that of their ligands (the decomposition temperature of btrz is 268 °C, while that of atrz is 292 °C, **Scheme 3**). Particularly, the onset decomposition temperature of **btrz-Zn** is more than 80 °C higher than that of **atrz-Zn** (283 °C). Thermogravimetric analyses further confirmed that the main loss weight (70%) of **btrz-Zn** is in the temperature range from 360 to 370 °C, while that (50%) of **atrz-Zn** is in the temperature range from 283 to 300 °C. The relatively high chemical and thermal stabilities of btrz-based CMOFs are possibly ascribed to their stronger M-N bonds between ligands and metal centers. The Cu-N bond lengths for **btrz-Cu** are 2.107 (4) Å, while those for **atrz-Cu** are 2.400(3) Å. The Zn-N bond lengths for **btrz-Zn** are 2.153 (3) Å, while those for **atrz-Zn** are 2.169(2) Å, (**Table S3**). Moreover, the stronger hydrogen-bonding interactions between the btrz ligand and charge-balanced ClO_4^- anions could also enhance stability (e.g., the C-H•••O hydrogen bonding distances are about 2.6333(139) Å for **btrz-Zn**, while those for **atrz-Zn** are about 2.7444(98) Å, **Table S4**).

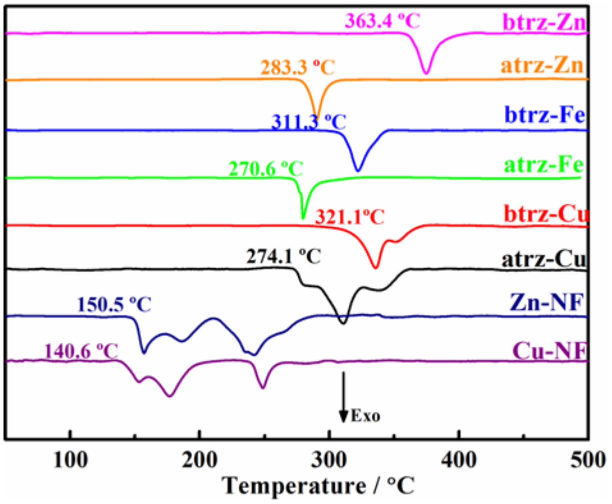

Figure 4. DSC curves for energetic CMOFs based on btrz and atrz.

Besides chemical stability and thermal stability, sensitivity also deserves significant attention from researchers because it is closely linked with the safety of handling and applying energetic materials. The impact and friction sensitivities of these CMOFs were measured using a BAM Fall Hammer BFH-10 and a FSKM-10 BAM friction apparatus, respectively. The impact sensitivities of **btrz-Zn**, **btrz-Cu**, **btrz-Fe**, **atrz-Zn**, **atrz-Cu**, and **atrz-Fe** are 26, 15, 11, 14, 9, and 2 J, respectively. The friction sensitivities of **btrz-Zn**, **btrz-Cu**, and **btrz-Fe**, are 52, 14, 48 N, respectively, while those of atrz-based CMOFs are less than 5 N. This indicates that btrz-based CMOFs are less sensitive than their corresponding atrz-based CMOFs. Compared with the rigid framework of atrz-based CMOFs, the flexible 3D framework of btrz-based

CMOFs absorbs more energy through the rotation of their N-N single bonds during impact or under friction, which could result in lower sensitivities.

(4) Detonation Properties. Since both btrz and atrz ligands have high heats of formation, and energetic ClO_4^- anions are employed as extra-framework anions, the detonation properties of their corresponding CMOFs were investigated. The heat of detonation (Q), regarded as the energy given off by an energetic material during detonation, is a critical performance metric. Following our developed method,[38] the heat of detonation of the energetic CMOFs were calculated using the experimentally determined enthalpy of formation (back-calculated from $-\Delta_cU$) and their corresponding measured density. As shown in **Table 1**, the heats of formation of btrz-based CMOFs are comparable to those of their atrz-based counterparts (e.g., 4997 kJ kg^{-1} for **btrz-Cu** vs 5006 kJ kg^{-1} for **atrz-Cu**; 5080 kJ kg^{-1} for **btrz-Zn** vs 5266 kJ kg^{-1} for **atrz-Zn**), and the azo groups could significantly enhance their heats of formation. Although btrz-based CMOFs have higher densities than their corresponding atrz-based CMOFs, atrz-based CMOFs possess higher heats of formation owing to their atrz content, which has higher heat of formation (878 kJ kg^{-1} for atrz *vs* 531 kJ kg^{-1} for btrz). This results in nearly equal heats of detonation between each pair.

Table 1. Physical properties of energetic CMOFs compared with their ligands and TNT.

Compd.	**T_d[a]**	**ρ[b]**	**Porosity[c]**	**Q[d]**	**$-\Delta_cU$[e]**	**$\Delta_fH°$[f]**	**IS[g]**	**FS[h]**
btrz	268	1.58 (1.59[i])	-	4421	-	531	>40	>360
atrz	292	1.64 (1.64[i])	-	5732	-	878	14	240
btrz-Cu	321	1.83 (1.83[i])	31.8%	4997	11580.9	1248	15	14
atrz-Cu	274	1.75 (1.81[i])	32.7%	5006	11116.4	1668	9	<5
btrz-Fe	312	1.82 (1.85 [i])	33.6%	5504	12309.7	1424	11	48
atrz-Fe	271	1.71 (1.76[i])	34.08%	5185	11225.7	1640	2	<5
btrz-Zn	363	1.81 (1.83 [i])	33.4%	5080	11646.9	1119	26	52
atrz-Zn	283	1.72 (1.74[i])	34.1%	5266	11104.0	1679	14	<5
Zn-NF	151	1.74 (1.77[i])	38.8%	5397	11567.4	1432	15.9	64
Cu-NF	140.6	1.74 (1.80[i])	38.2%	5330	11458.9	1341	9.5	72
TNT	290	1.71	-	5258	-	1651	15	353

[a] Decomposition temperature (onset), °C. [b] Density measured by gas pycnometer, g cm^{-3}. [c] Porosity calculated by Platon software. [d] Heat of detonation, kJ kg^{-1}. [e] Experimental determined (oxygen bomb calorimetry) contant volume energy of combustion (kJ kg^{-1})[f] Heat of detonation, kJ mol^{-1} [g] Impact sensitivity, J. [h] Frication sensitivity, N. [i] Crystal densities, g cm^{-3}.

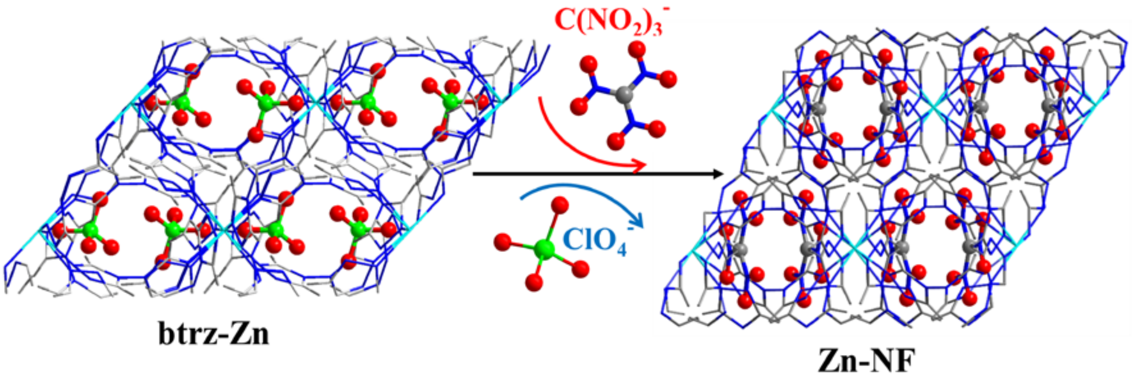

Figure 5. (Left) Crystal packing of **btrz-Zn**. (Right) Crystal packing of **Zn-NF**. The scheme is shown for the exchange process of trapping $C(NO_2)_3^-$ anions and loss of ClO_4^- anions.

2. Effect of anionic group on the properties of energetic CMOFs

(1) Synthesis and Structure. To assess the influence of energetic anionic groups on the properties of CMOFs, we employed as-prepared btrz-based CMOFs as precursors to synthesize two new energetic CMOFs containing extra-framework, $C(NO_2)_3^-$ anions, through anion exchange. Since btrz-based CMOFs have high chemical stabilities; moreover, ClO_4^- as extra-framework mobile anions occupy the framework channels and are uncoordinated to the metal centers, which facilitaties anion exchange. Accordingly, an anion-exchange experiment was performed. After white crystals of **btrz-Zn** were immersed in a $KC(NO_2)_3$ solution under static ambient conditions (room temperature) for 3 days, they turned yellow (**Figure S17**), revealing quantitatively new crystals ($\{[Zn(btr)_3](NF)_2\}_n$, **Zn-NF**), as illustrated in **Figure 5**. An infrared (IR) spectrum of the solid product showed a strong band associated with the $C(NO_2)_3^-$ anion (~1300 cm^{-1}), along with the disappearance of band of ClO_4^- anion (~1100 cm^{-1}) (**Figure S16b**). The whole exchange process was monitored visually, and no crystal dissolution was observed. Notably, the resultant MOF remained single crystalline, was heterogeneous throughout the exchange at the bottom of the aqueous solution and could be gathered through simple filtration. PXRD and single-crystal diffraction analyses indicated that as-prepared **Zn-NF** is isostructural to **btrz-Zn**, except that the extra-framework ClO_4^- anions were substituted by $C(NO_2)_3^-$ (**Figure 5** and **Figure S13**). In addition, **Cu-NF** $\{[Cu(btr)_3](NF)_2\}_n$ was synthesized in a similar manner as Zn-NF, except that **btrz-Cu** was used instead of **btrz-Zn**. PXRD and single-crystal diffraction analyses showed that **Cu-NF** (**Figure S12**) is isostructural to both **btrz-Cu** and **Zn-NF**.

(2) Energetic Properties. As shown from **Figure 6**, although perchlorate-based CMOFs (the precursors) and their corresponding nitroformate-based CMOFs have the same backbones, the former exhibited higher densities. In particular, the density of **btrz-Cu** is 0.09 g cm^{-3} more than that of **Cu-NF** (1.83 g cm^{-3} for **btrz-Cu** vs 1.74 g cm^{-3} for **Cu-NF**). The extra-framework perchlorate anion has a higher density compared to the $C(NO_2)_3^-$ anion [2.52 g cm^{-3} for $KClO_4$ *vs* 2.22 g cm^{-3} for $KC(NO_2)_3$], which could result in their corresponding CMOFs having higher densities. In addition, perchlorate-based CMOFs also displayed higher thermal stabilities than their corresponding nitroformate-based CMOFs. Remarkably, the decomposition temperature of **btrz-Zn** is more than 200 °C higher than that of **Zn-NF** (**Figure 4,** 363 °C for **btrz-Zn** *vs* 151 °C for **Zn-NF**). The relatively low thermal stabilities of nitroformate-based CMOFs are mainly ascribed to their labile $C(NO_2)_3^-$ anion content. It is well-known that nitroformate salts usually have poor thermal stabilities [e.g., the decomposition temperature of $KC(NO_2)_3$ is 83 °C, while that of $KClO_4$ is 400 °C]. However, since the $C(NO_2)_3^-$ anion has high nitrogen and oxygen contents, the nitroformate-based CMOFs possess higher heats of detonation than their counterparts containing ClO_4^- anions (e.g., 5397 kJ kg^{-1} for **Zn-NF** vs 5080 kJ kg^{-1} for **btrz-Zn**). Therefore, the effect of anionic groups on the properties of CMOFs follows the traditional energetic group law.

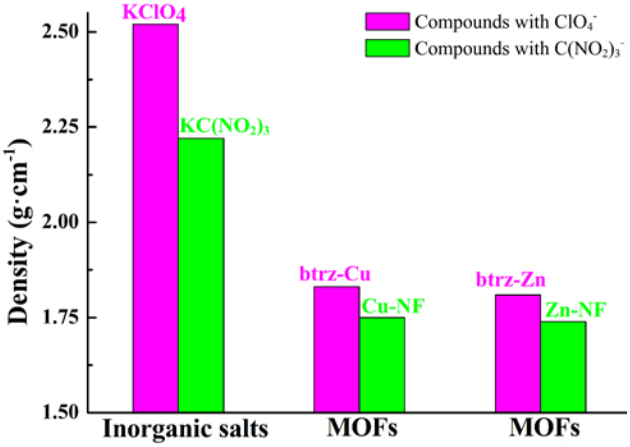

Figure 6. Densities comparison for $KClO_4$, $KC(NO_2)_3$, and perchlorate-based CMOFs and nitroformate-based CMOFs with the same cationic frameworks.

Conclusion

We successfully fabricated a series of energetic CMOFs system to firstly investigate its structure-property relationship in them. Two kinds of CMOFs having similar structure, btrz- and atrz-based CMOFs, were synthesized. As a result, the effect of ligand backbones on their densities and stabilities were discovered to be inverse that of backbones in traditional energetic compounds. However, the effect of the anionic group on CMOFs still follows the traditional group law. We found that btrz-based CMOFs exhibit higher densities and better stabilities than those of their corresponding counterparts, although btrz has a lower density and stability than atrz. In particular, the density of **btrz-Fe** is more than 0.11 g cm^{-3} higher than that of its atrz-based analogue (**atrz-Fe**). Moreover, the decomposition temperature of **btrz-Zn** (363 °C) is more than 80 °C higher than that of **atrz-Zn**, even higher than that of **TATB**, making it a potential heat-resistant explosive. Mechanistic studies showed that btrz-based CMOFs have lower porosities and smaller channels, resulting in higher densities. Moreover, the stronger M-N bonds and hydrogen-bonding interactions lead to their higher stabilities. Traditionally, the densities of energetic compounds mainly depend on backbones and energetic groups. Here, the size of channels and total empty volume of the frameworks were proven to be equally influential. Therefore, this investigation produced meaningful understanding of the structure-property relationship in energetic CMOFs. Moreover, our study also brings about new insight for the design and synthesis of new high-performance energetic materials.

Experimental Section

Caution: Although it is not encountered in our experiments, perchlorate and nitroformate anions contained compounds are potentially explosive. Only a small amount of the materials should be prepared, and it should be handled with care.

General methods. All starting materials were commercially available, reagent grade, and used as purchased without further purification. The ligands btrz and atrz were prepared according to the method in the literature.[39, 40] FT-IR spectra were recorded using KBr pellets for solids on a Bruker Tensor 27 spectrometer. DSC studies were performed on a TA-DSC Q2000 (New Castle, DE, USA) with the heating rate of 10 °C min^{-1}, the flow rate of nitrogen gas of 60 mL min^{-1}, and the sample size of about 1.0 mg. The absolute density of eight complexes were measured using an automatic gas pycnometer (Ultrapyc 1200e, Quantachrome Instruments). The impact and friction sensitivities were performed on a BAM fall hammer BFH-10 and a BAM friction apparatus FSKM-10, respectively. Detonation pressures and velocities were predicted based on the Chapman-Jouget thermodynamic detonation theory using EXPLO 6.01 and the Kamlet-Jacobs equation.

Synthesis of btrz-Cu, btrz-Fe, atrz-Zn and atrz-Fe. btrz-Cu, **btrz-Fe**, **atrz-Zn** and **atrz-Fe** were synthesized according to the reference methods.[24, 25, 41, 42]

Synthesis of $[Cu(atrz)_3](ClO_4)_2$ (atrz-Cu). atrz (1.5 mmol, 0.246 g) in 20 mL of boiling water was added into a boiling aqueous solution of 20 mL $Cu(ClO_4)_2.6H_2O$ (0.5 mmol, 0.185 g). The mixture was stirred for 1 h, and then filtered. Blue single-crystals suitable for X-ray diffraction were obtained by slow evaporation in a glass vial within several days with a yield of 79%.

Synthesis of $[\mathrm{Zn(btr)_3}](\mathrm{ClO_4})_2$(btrz-Zn). btrz (1.0 mmol, 0.136 g) in 20 mL of water was added into a 20 mL $\mathrm{Zn(ClO_4)_2.6H_2O}$ (0.5 mmol, 0.185 g) aqueous solution. The mixture was then filtered. Transparent single-crystals suitable for X-ray diffraction were obtained by slow evaporation in a glass vial within several days with a yield of 83%.

Synthesis of $[\mathrm{Zn(btrz)_3}](\mathrm{NF})_2$. (Zn-NF). As-synthesized btrz-Zn (0.3 mmol) crystals were immersed in a 20 ml $\mathrm{KC(NO_2)_3}$ (0.9 mmol) aqueous solution for 3 days. Yellow block crystals of **Zn-NF** suitable for X-ray diffraction were obtained. After decanting the solution, the resultant solids were washed thoroughly with deionized water, and then dried in vacuum at 60 °C for 24 h. The products were characterized by PXRD and IR spectroscopy. Results are shown in the Supporting Information.

Synthesis of $[\mathrm{Cu(btrz)_3}](\mathrm{NF})_2$. (Cu-NF). The synthetic procedure and reactant amount for **Cu-NF** were the same as those for **Zn-NF** except that **btrz-Zn** was replaced by **btrz-Cu**. The obtained crystals for **Cu-NF** were green and were also characterized by PXRD and IR spectroscopy. The results are listed in the Supporting Information.

Single-Crystal X-ray Crystallography. Single Crystal X-ray diffraction data were collected using a Bruker-AXS SMART APEX2 CCD diffractometer (Mo Kα, λ= 0.71073 Å). Indexing was performed using APEX2 (Difference Vectors method). Data integration and reduction were performed using SaintPlus. Absorption correction was performed by multiscan method implemented in SADABS. Space groups were determined using XPREP implemented in APEX2. Structures were solved using SHELXL-97 (direct methods) and refined using SHELXL-97 (full-matrix least-squares on F2) with anisotropic displacement contained in APEX2 program packages. Hydrogen atoms on carbon and nitrogen and oxygen were calculated in ideal positions with isotropic placement parameters set to 1.2 × Ueq of the attached atoms. CCDC 1570227, 1570245, 1571481, and 1571482 contain the supplementary crystallographic data for this paper. These data can be obtained free of charge from The Cambridge Crystallographic Data Centre via www.ccdc.cam.ac.uk/data_request/cif.

ASSOCIATED CONTENT

Supporting Information. The Supporting Information is available free of charge via the Internet at http://pubs.acs.org.

AUTHOR INFORMATION

Corresponding Authors

* E-mail: lishenghua@bit.edu.cn.

* E-mail: pangsp@bit.edu.cn.

Notes

The authors declare no competing financial interest.

ACKNOWLEDGMENT

The authors acknowledge financial support from NSAF (U1530262), the National Natural Science Foundation of China (21576026), and the Fundamental Research Funds for the Central Universities.

REFERENCES

(1) Chen, W.-C.; Yuan, Y.; Xiong, Y.; Rogach, A. L.; Tong, Q.-X.; Lee, C.-S. Aromatically C6- and C9- Substituted Phenanthro [9, 10-d] imidazole Blue Fluorophores: Structure–Property Relationship and Electroluminescent Application. *ACS Appl. Mater. Interfaces* **2017,** 9, 26268-26278.

(2) Zhang, J.; Xu, W.; Sheng, P.; Zhao, G.; Zhu, D. Organic Donor–Acceptor Complexes as Novel Organic Semiconductors. *Acc. Chem. Res.* **2017,** 50, 1654-1662.

(3) Bazban-Shotorbani, S.; Hasani-Sadrabadi, M. M.; Karkhaneh, A.; Serpooshan, V.; Jacob, K. I.; Moshaverinia, A.; Mahmoudi, M. Revisiting structure-property relationship of pH-responsive polymers for drug delivery applications. *J. Controlled Release* **2017,** 253, 46-63.

(4) Laveda, J. V.; Johnston, B.; Paterson, G. W.; Baker, P. J.; Tucker, M. G.; Playford, H. Y.; Jensen, K. M.; Billinge, S. J.; Corr, S. A. Structure–property insights into nanostructured electrodes for Li-ion batteries from local structural and diffusional probes. *J. Mater. Chem. A* **2018,** 6, 127-137.

(5) Zeng, S.; Zhang, X.; Bai, L.; Zhang, X.; Wang, H.; Wang, J.; Bao, D.; Li, M.; Liu, X.; Zhang, S. Ionic-liquid-based CO2 capture systems: structure, interaction and process. *Chem. Rev.* **2017,** 117, 9625-9673.

(6) Willis, J. J.; Gallo, A.; Sokaras, D.; Aljama, H.; Nowak, S. H.; Goodman, E. D.; Wu, L.; Tassone, C. J.; Jaramillo, T. F.; Abild-Pedersen, F. Systematic Structure–Property Relationship Studies in Palladium-Catalyzed Methane Complete Combustion. *ACS Catalysis* **2017,** 7, 7810-7821.

(7) Göbel, M.; Klapötke, T. M. Development and testing of energetic materials: the concept of high densities based on the trinitroethyl functionality. *Adv. Funct. Mater.* **2009,** 19, 347-365.

(8) Yin, P.; Mitchell, L. A.; Parrish, D. A.; Shreeve, J. M. Energetic N-Nitramino/N-Oxyl-Functionalized Pyrazoles with Versatile π–π Stacking: Structure–Property Relationships of High-Performance Energetic Materials. *Angew. Chem. Int. Ed.* **2016,** 55, 14409-14411.

(9) Dippold, A. A.; Klapötke, T. M. A study of dinitro-bis-1, 2, 4-triazole-1, 1′-diol and derivatives: design of high-performance insensitive energetic materials by the introduction of N-oxides. *J. Am. Chem. Soc.* **2013,** 135, 9931-9938.

(10) Zhao, X.; Li, S.; Wang, Y.; Li, Y.; Zhao, F.; Pang, S. Design and synthesis of energetic materials towards high density and positive oxygen balance by N-dinitromethyl functionalization of nitroazoles. *J. Mater. Chem. A* **2016,** 4, 5495-5504.

(11) Yin, P.; Zhang, Q.; Shreeve, J. M. Dancing with energetic nitrogen atoms: Versatile N-functionalization strategies for N-heterocyclic frameworks in high energy density materials. *Acc. Chem. Res.* **2015,** 49, 4-16.

(12) Talawar, M.; Sivabalan, R.; Mukundan, T.; Muthurajan, H.; Sikder, A.; Gandhe, B.; Rao, A. S. Environmentally compatible next generation green energetic materials (GEMs). *J. Hazard. Mater.* **2009,** 161, 589-607.

(13) Klapötke, T. M.; Mayer, P.; Miró Sabaté, C.; Welch, J. M.; Wiegand, N. Simple, nitrogen-rich, energetic salts of 5-nitrotetrazole. *Inorg. Chem.* **2008,** 47, 6014-6027.

(14) Zhang, Q.; Shreeve, J. M. Metal–organic frameworks as high explosives: A new concept for energetic materials. *Angew. Chem. Int. Ed.* **2014,** 53, 2540-2542.

(15) Liu, X.; Gao, W.; Sun, P.; Su, Z.; Chen, S.; Wei, Q.; Xie, G.; Gao, S. Environmentally friendly high-energy MOFs: crystal structures, thermostability, insensitivity and remarkable detonation performances. *Green Chemistry* **2015,** 17, 831-836.

(16) Zhang, J. H.; Shreeve, J. M. 3D Nitrogen-rich metal-organic frameworks: opportunities for safer energetics. *Dalton Trans.* **2016,** 45, 2363-2368.

(17) Zhang, S.; Yang, Q.; Liu, X.; Qu, X.; Wei, Q.; Xie, G.; Chen, S.; Gao, S. High-energy metal–organic frameworks (HE-MOFs): Synthesis, structure and energetic performance. *Coord. Chem. Rev.* **2016,** 307, 292-312.

(18) Li, S.; Wang, Y.; Qi, C.; Zhao, X.; Zhang, J.; Zhang, S.; Pang, S. 3D Energetic Metal–Organic Frameworks: Synthesis and Properties of High Energy Materials. *Angew. Chem. Int. Ed.* **2013,** 52, 14031-14035.

(19) Xu, J.-G.; Sun, C.; Zhang, M.-J.; Liu, B.-W.; Li, X.-Z.; Lu, J.; Wang, S.-H.; Zheng, F.-K.; Guo, G.-C. Coordination Polymerization of Metal Azides and Powerful Nitrogen-Rich Ligand toward Primary Explosives with Excellent Energetic Performances. *Chem. Mater.* **2017,** 29, 9725-9733.

(20) Li, W.; Wang, K.; Qi, X.; Jin, Y.; Zhang, Q. Construction of a Thermally Stable and Highly Energetic Metal–Organic Framework as Lead-Free Primary Explosives. *Cryst. Growth Des.* **2018,** 18, 1896-1902.

(21) Zhang, J.; Du, Y.; Dong, K.; Su, H.; Zhang, S.; Li, S.; Pang, S. Taming dinitramide anions within an energetic metal–organic framework: A new strategy for synthesis and tunable properties of high energy materials. *Chem. Mater.* **2016,** 28, 1472-1480.

(22) Blair, L.; Colakel, A.; Vrcelj, R.; Sinclair, I.; Coles, S. Metal–organic fireworks: MOFs as integrated structural scaffolds for pyrotechnic materials. *Chem. Commun.* **2015,** 51, 12185-12188.

(23) McDonald, K. A.; Seth, S.; Matzger, A. J. Coordination polymers with high energy density: An emerging class of explosives. *Cryst. Growth Des.* **2015,** 15, 5963-5972.

(24) Zhang, J.; Su, H.; Dong, Y.; Zhang, P.; Du, Y.; Li, S.; Gozin, M.; Pang, S. Synthesis of Denser Energetic Metal–Organic Frameworks via a Tandem Anion–Ligand Exchange Strategy. *Inorg. Chem.* **2017,** 56, 10281-10289.

(25) Huang, Y.-Q.; Zhao, X.-Q.; Shi, W.; Liu, W.-Y.; Chen, Z.-L.; Cheng, P.; Liao, D.-Z.; Yan, S.-P. Anions-directed metal-mediated assemblies of coordination polymers based on the bis (4, 4′-bis-1, 2, 4-triazole) ligand. *Cryst. Growth Des.* **2008,** 8, 3652-3660.

(26) Ding, B.; Wang, Y. Y.; Liu, S. X.; Wu, X. X.; Zhu, Z. Z.; Huo, J. Z.; Liu, Y. Y. A series of multi-dimensional metal–organic frameworks with trans-4, 4′-azo-1 ,2, 4-triazole: polymorphism, guest induced single-crystal-to-single-crystal transformation and solvatochromism. *CrystEngComm* **2015,** 17, 5396-5409.

(27) Qi, C.; Li, S.-H.; Li, Y.-C.; Wang, Y.; Chen, X.-K.; Pang, S.-P. A novel stable high-nitrogen energetic material: 4, 4′-azobis (1, 2, 4-triazole). *J. Mater. Chem.* **2011,** 21, 3221-3225.

(28) Chuang, Y.-C.; Ho, W.-L.; Sheu, C.-F.; Lee, G.-H.; Wang, Y. Crystal engineering from a 1D chain to a 3D coordination polymer accompanied by a dramatic change in magnetic properties. *Chem. Commun.* **2012,** 48, 10769-10771.

(29) Bartlett, R.; Humphrey, I. Transaminations of NN-dimethylformamide azine. *J. Chem. Soc. C* **1967,** 1664-1666.

(30) Miyata, Y.; Baba, K.; Date, S.; Hasue, K. Performance evaluation of gas generating agents based on 5-amino-1H-tetrazole/oxidizer mixtures by using closed vessel test. *Sci. Technol. Energ. Ma.* **2004,** 65, 167-172.

(31) Göbel, M.; Klapötke, T. M.; Mayer, P. Crystal structures of the potassium and silver salts of nitroform. *Z. Anorg. Allg. Chem.* **2006,** 632, 1043-1050.

(32) Spek, A. PLATON, A Multipurpose Crystallographic Tool; Utrecht University: Utrecht, The Netherlands, 2003.

(33) Kamlet, M. J.; Jacobs, S. Chemistry of detonations. I. A simple method for calculating detonation properties of C–H–N–O explosives. *J. Chem. Phys.* **1968,** 48, 23-35.

(34) Jiang, H.-L.; Feng, D.; Wang, K.; Gu, Z.-Y.; Wei, Z.; Chen, Y.-P.; Zhou, H.-C. An exceptionally stable, porphyrinic Zr metal–organic framework exhibiting pH-dependent fluorescence. *J. Am. Chem. Soc.* **2013,** 135, 13934-13938.

(35) Feng, D.; Gu, Z.-Y.; Chen, Y.-P.; Park, J.; Wei, Z.; Sun, Y.; Bosch, M.; Yuan, S.; Zhou, H.-C. A highly stable porphyrinic zirconium metal–organic framework with shp-a topology. *J. Am. Chem. Soc.* **2014,** 136, 17714-17717.

(36) Wang, B.; Lv, X.-L.; Feng, D.; Xie, L.-H.; Zhang, J.; Li, M.; Xie, Y.; Li, J.-R.; Zhou, H.-C. Highly Stable Zr(IV)-Based Metal-Organic Frameworks for the Detection and Removal of Antibiotics and Organic Explosives in Water. *J. Am. Chem. Soc.* **2016,** 138, 6204-6216.

(37) Zhang, Y. Q.; Guo, Y.; Joo, Y. H.; Parrish, D. A.; Shreeve, J. M. 3,4,5-Trinitropyrazole-Based Energetic Salts. *Chem.-Eur. J.* **2010,** 16, 10778-10784.

(38) Wang, Y.; Zhang, J.; Su, H.; Li, S.; Zhang, S.; Pang, S. A simple method for the prediction of the detonation performances of metal-containing explosives. *J. Phys. Chem. A* **2014,** 118, 4575-4581.

(39) Naik, A. D.; Marchand-Brynaert, J.; Garcia, Y. A simplified approach to N-and N, N′-linked 1, 2, 4-triazoles by transamination. *Synthesis* **2008,** 2008, 149-154.

(40) Li, S. H.; Pang, S. P.; Li, X. T.; Yu, Y. Z.; Zhao, X. Q. Synthesis of new tetrazene(N-N=N-N)-linked bi(1,2,4-triazole) *Chin. Chem. Lett.* **2007,** 18, 1176-1178.

(41) Garcia, Y.; Kahn, O.; Rabardel, L.; Chansou, B.; Salmon, L.; Tuchagues, J. P. Two-Step Spin Conversion for the Three-Dimensional Compound Tris(4,4‘-bis-1,2,4-triazole)iron(II) Diperchlorate. *Inorg. Chem.* **1999,** 38, 4663-4670.

(42) Chuang, Y.-C.; Liu, C.-T.; Sheu, C.-F.; Ho, W.-L.; Lee, G.-H.; Wang, C.-C.; Wang, Y. New Iron(II) Spin Crossover Coordination Polymers $[Fe(\mu\text{-atrz})_3]X_2{\cdot}2H_2O$ (X = ClO_4^-, BF_4^-) and $[Fe(\mu\text{-atrz})(\mu\text{-pyz})(NCS)_2]{\cdot}4H_2O$ with an Interesting Solvent Effect. *Inorg. Chem.* **2012,** 51, 4663-4671.

For Table of Contents Only

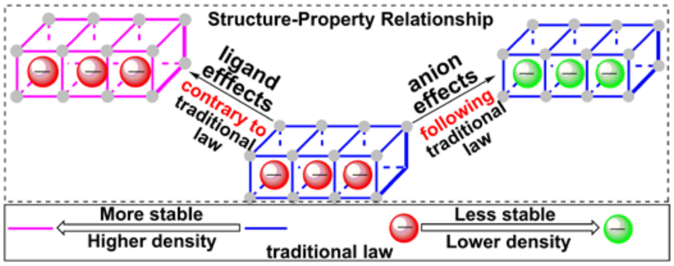

The structure-property relationships about ligand effect and counter anion effect of energetic cationic metal-organic frameworks are revealed for the first time. The results show that the effect of ligand backbones on these energetic CMOFs is inverse that of the backbones on traditional energetic compounds, while the effect of the anionic groups on CMOFs still follows the traditional group law.

Keyword: cationic metal organic frameworks, structure-property relationship, anion exchange, energetic materials

Yao Du, Hui Su, Teng Fei, Baoping Hu, Jichuan Zhang, Shenghua Li*, Siping Pang* and Fude Nie

Structure-Property Relationship in Energetic Cationic Metal–Organic Frameworks: New Insight for Design of Advanced Energetic Materials

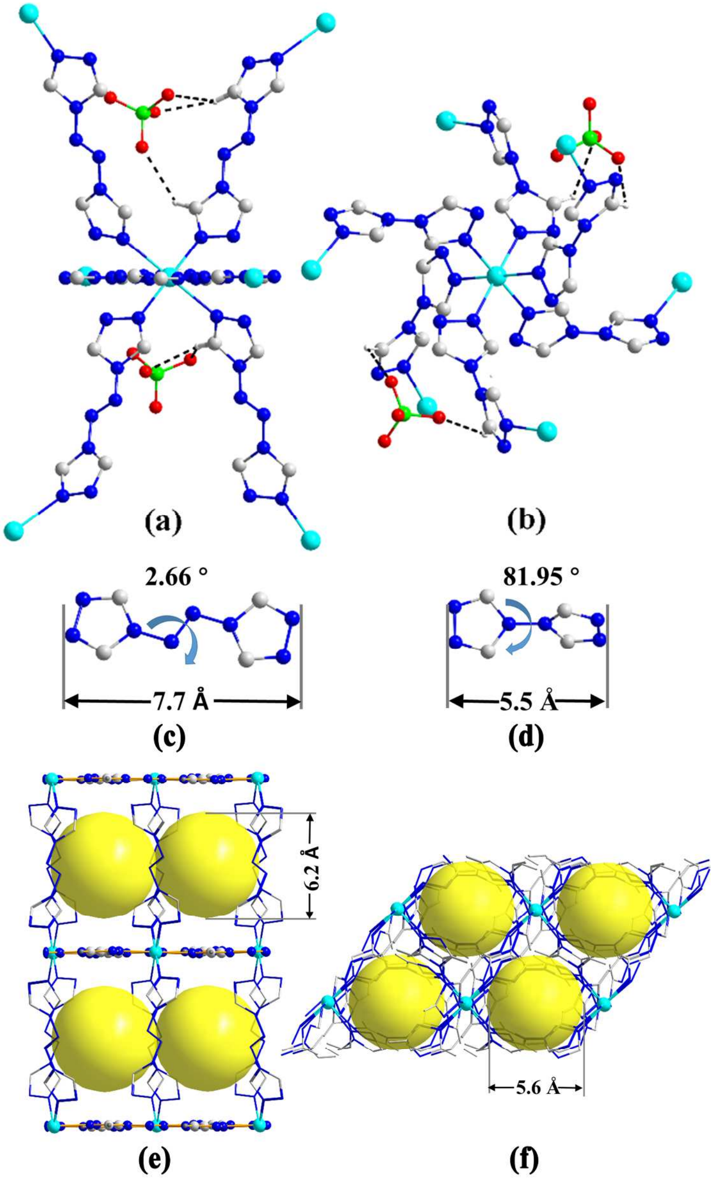

Figure 1. Coordination environment of Zn in **atrz-Zn** (a). Coordination environment of Zn in **btrz-Zn** (b). Structure for ligand atrz in **atrz-Zn** (c). Structure for ligand btrz in **btrz-Zn** (d). 3D frameworks of **btrz-Zn** (e). 3D frameworks of **atrz-Zn** (f). Some charge-balancing anions, hydrogen atoms, and guest water are omitted for clarity. The large spheres indicate the size of the voids.

162x266mm (300 x 300 DPI)

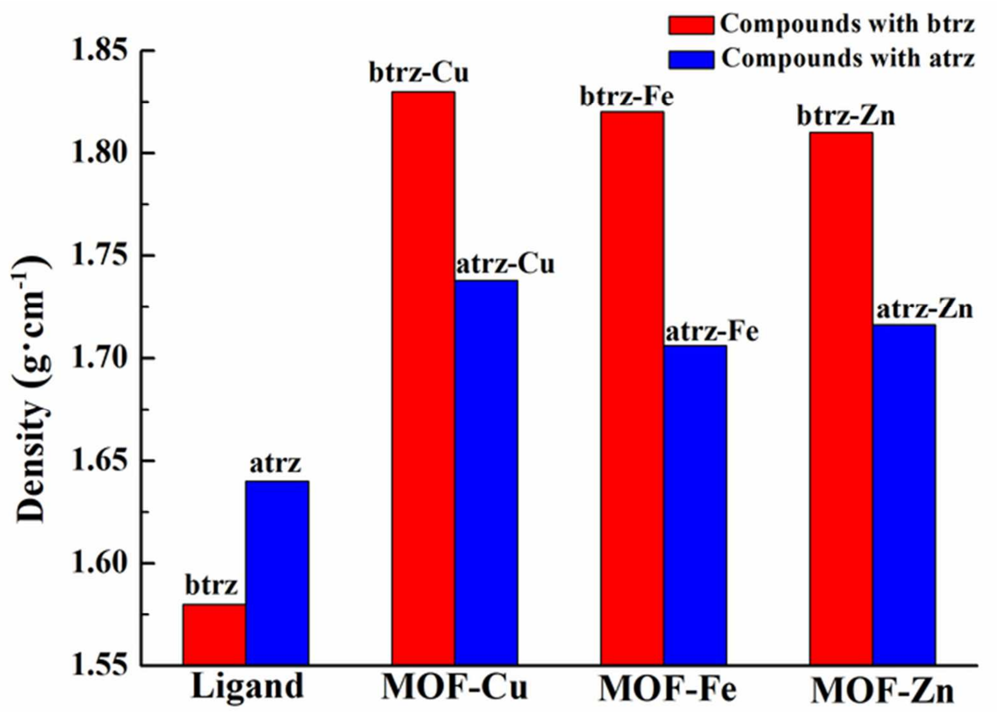

Figure 2. Densities comparison for btrz, atrz and their atrz-based CMOFs and btrz-based CMOFs with the same extra-framework ClO4¯ anions.

59x42mm (300 x 300 DPI)

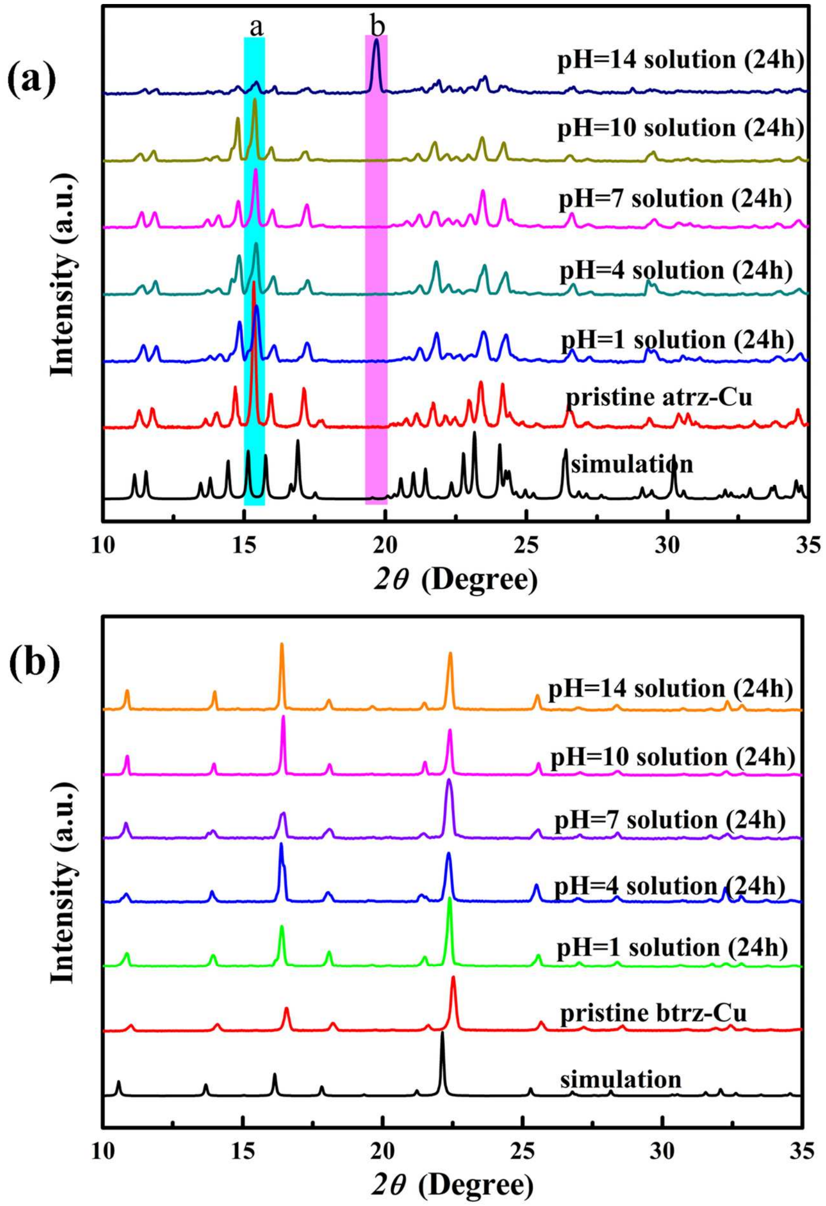

Figure 3. PXRD profiles for simulated and experimental **atrz-Cu** (a) and **btrz-Cu** (b) samples soaked in aqueous solutions with pH values of 1, 4, 7, 10 and 14 for 24 h.

109x156mm (300 x 300 DPI)

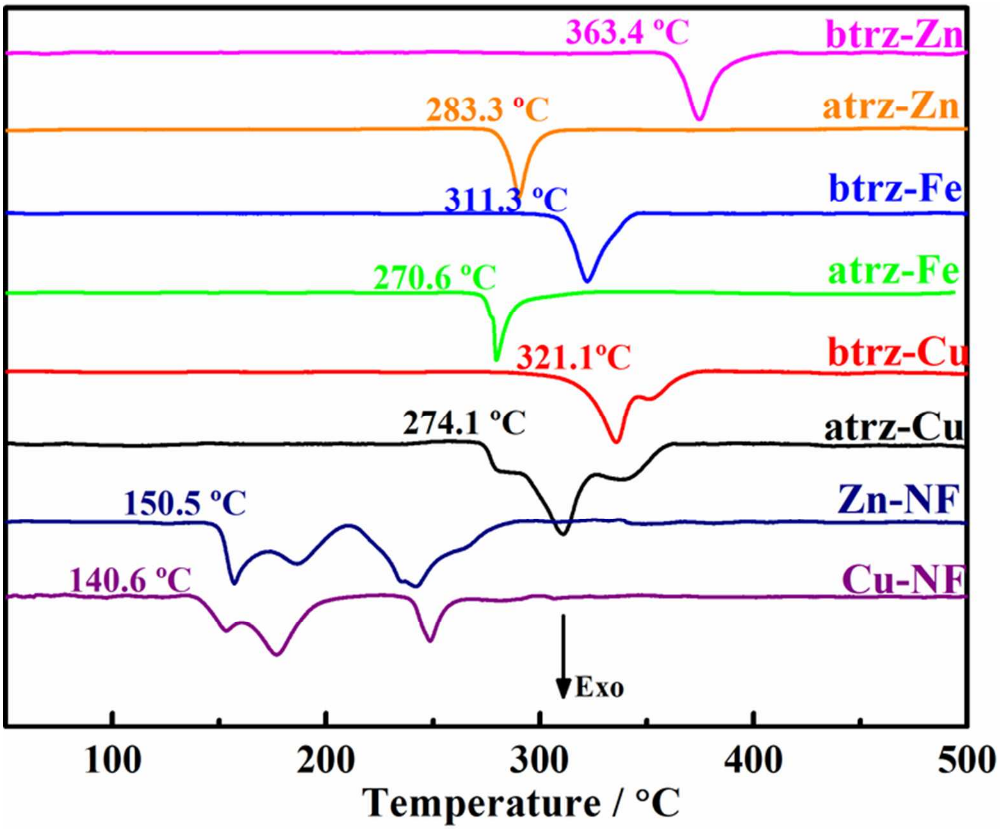

Figure 4. DSC curves for energetic CMOFs based on btrz and atrz.

65x54mm (300 x 300 DPI)

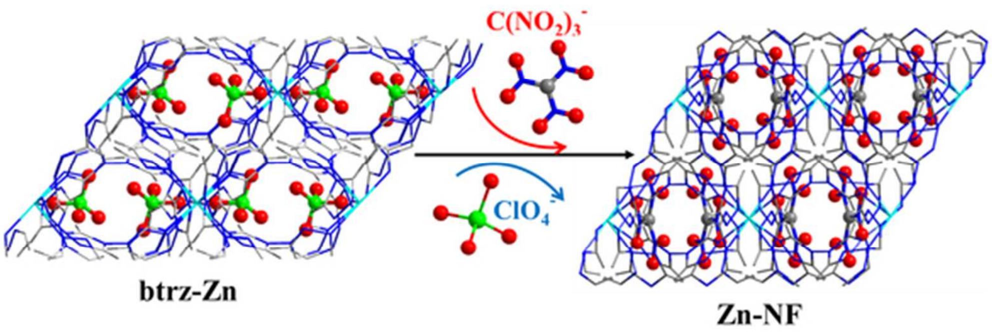

Figure 5. (Left) Crystal packing of **btrz-Zn**. (Right) Crystal packing of **Zn-NF**. The scheme is shown for the exchange process of trapping $C(NO_2)_3^-$ anions and loss of ClO_4^- anions.

49x16mm (300 x 300 DPI)

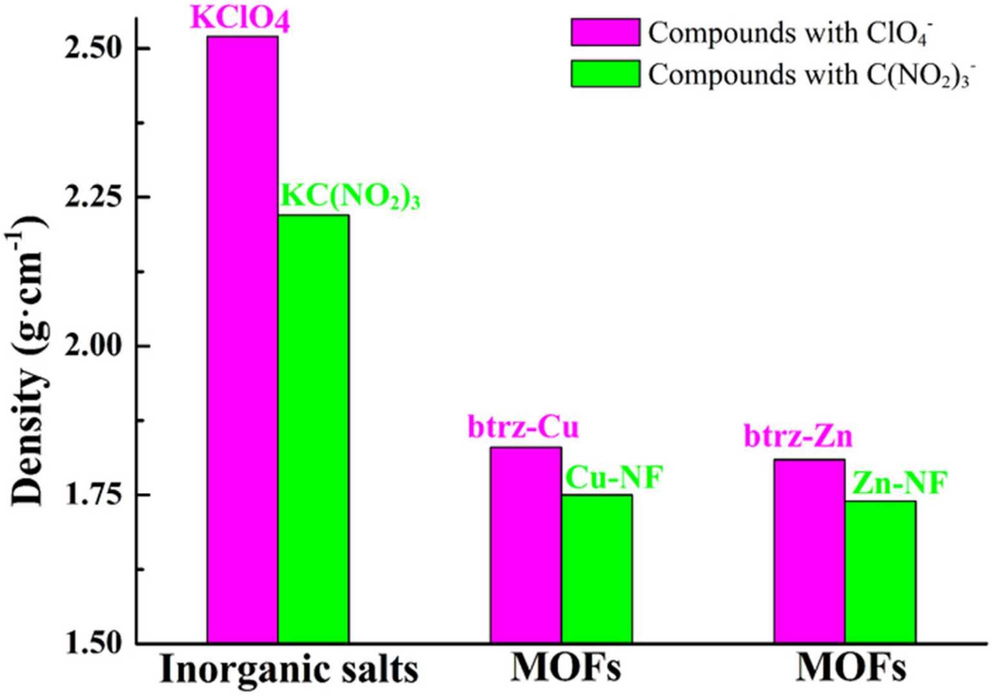

Figure 6. Densities comparison for $KClO_4$, $KC(NO_2)_3$, and perchlorate-based CMOFs and nitroformate-based CMOFs with the same cationic frameworks.

59x42mm (300 x 300 DPI)

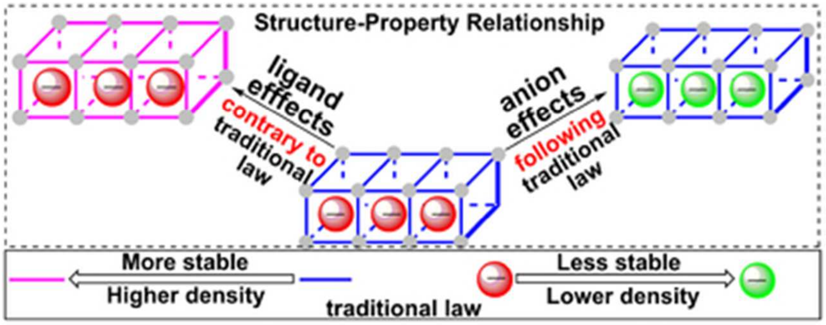

TOC

34x13mm (300 x 300 DPI)